Polymers **2015**, *7*, 1577-1586; doi:10.3390/polym7081471

OPEN ACCESS

polymers

ISSN 2073-4360

www.mdpi.com/journal/polymers

Article

Controllable Direct-Writing of Serpentine Micro/Nano Structures via Low Voltage Electrospinning

Feiyu Fang, Xin Chen, Zefeng Du, Ziming Zhu, Xindu Chen, Han Wang * and Peixuan Wu *

Guangdong Provincial Key Laboratory of Micro-Nano Manufacturing Technology and Equipment, Guangdong University of Technology, Guangzhou 510006, China;
E-Mails: feiyu93@foxmail.com (F.F.); chenx@gdut.edu.cn (XinC.); zefengdut@foxmail.com (Z.D.); Sevident_zhu@163.com (Z.Z.); xinduchengdut@163.com (Xind.C.)

* Authors to whom correspondence should be addressed; E-Mails: wanghangdut@126.com (H.W.); peixuan@gdut.edu.cn (P.W.); Tel.: +86-20-2388-0655 (H.W.).

Academic Editor: Scott M. Husson

Received: 20 July 2015 / Accepted: 14 August 2015 / Published: 24 August 2015

Abstract: Micro/nanofibers prepared by direct-writing using an electrospinning (ES) technique have drawn more attention recently owing to their intriguing physical properties and great potential as building blocks for micro/nanoscale devices. In this work, a wavy direct-writing (WDW) process was developed to directly write serpentine micro/nano structures suitable for the fabrication of micro devices. This fabrication ability will realize the application of electrospun-nanofiber-based wiring of structural and functional components in microelectronics, MEMS, sensor, and micro optoelectronics devices, and, especially, paves the way for the application of electrospinning in printing serpentine interconnector of large-area organic stretchable electronics.

Keywords: electrospinning; direct-writing; serpentine structure; micro pattern

---

1. Introduction

Serpentine structures are common in our daily life and are found in many diverse systems, including antennas, heating pipes, tube type radiators, and lights. Due to their excellent mechanical and electrical properties and performance, serpentine structures show enormous potential for applications in many areas, such as epidermal electronics [1], curvilinear digital cameras [2], stretchable batteries [3], and light-emitting devices [4]. Of special note, it has been reported that stretchable batteries with self-similar

serpentine interconnects enable reversible levels of stretch ability as high as 300% [3] and the substantial resistive strain sensitivity reduction (~1100%) with the encapsulated serpentine pattern [5].

Conventional methods, such as electron beam lithography, focused ion beams (FIB), and dip-pen nanolithography (DPN), are capable of generating well-defined micro/nano patterns [6–8], but they are inefficient and require special equipment and complex processes. Inkjet printing is an attractive method of depositing patterns while the minimum reliable printing resolution ranges from 20 to 30 μm [9]. A size limitation, which prevents the fabrication of smaller patterns, does exist. Electrohydrodynamic (EHD) printing is a technique that has the potential to print high resolution patterns [10]. However, due to the discontinuous feature, precise continuous patterning is still unable to be achieved with EHD printing. Thus, there is a significant need to produce continuous serpentine structures in a simpler, more cost-effective way.

The efficiency and low-cost production of micro/nanostructures by electrospinning (ES) via a direct-writing process has gained popularity recently, owing to its enormous potential for application in many areas including light-emitters [11,12], field-effect transistors [13], piezoelectric devices [14], and supercapacitors [15]. ES is considered to be a straightforward, low-cost technique to fabricate ultra-thin fibers with diameters ranging from tens of nanometers to several micrometers [16,17]. In particular, having the ability to deposit functional materials directly and without contact on a variety of substrates, including flexible substrates, ES can be used to directly print large-area organic semiconducting nanowire arrays on device substrates, enabling sophisticated large-area nanowire lithography for nanoelectronics [18,19]. Thus, ES is considered to be a promising alternative to traditional lithography technology to produce microelectronic devices in an ingenious and cost-effective way.

While a conventional ES system is simple, the physics of the process is extremely complex. Owing to the bending instability of a charged jet under coupled multi-field forces, the ES process is unstable and almost uncontrollable. A revolutionary technology breakthrough has been developed to increase the controllability of a single fiber by shortening the needle-to-collector distance. This improved process, near-field electrospinning (NFES), has been developed to write smooth microfibers in a direct manner [20]. However, a challenge to precisely write different patterns using NFES still exists [21]. In order to obtain a specific serpentine/helical structure to meet the requirements for the manufacture of micro/nano devices, several exploratory studies have been carried out, yielding remarkable results [22–27]. However, challenges remain in producing micro/nano scale serpentine patterns stably, where frequency, amplitude, and wavelength can be control precisely.

In this study, we developed the wavy direct-writing (WDW) process, a simple but effective method, to directly write high-resolution serpentine patterns. This fabrication ability has potential application in many fields, including stretchable energy harvesters [28,29], stretchable strain sensors [24], light-emitters [12,30], photonics, electronics, and micromechanics [31].

2. Experimental Section

Polyethylene oxide (PEO) with an average molecular weight of 2,000,000 (Aladdin, Shanghai, China) was chosen for the preparation of the solutions. PEO fibers were electrospun using 3%–8% (*w*/*w*) concentrations of PEO in deionized water with 4 h stirring at 20 °C. The ground collector

was made of chromium-plated glass. The PEO solution was delivered with a syringe pump (Lange, Inc., Baoding, China).

The schematic diagram of the wavy direct-writing (WDW) apparatus is shown in Figure 1. A stainless steel nozzle (inner diameter 260 μm and external diameter 520 μm) was adopted as an electrode, and the ground collector was a Cr-coated glass plate fixed to a moving stage (Suruga, Shizuoka, Japan). A high voltage, generated by a direct current (DC) power supply (DW-P403, Dongwen Inc., Tianjin, China), was applied between the nozzle and the collector to generate a Taylor cone to assist in pulling out the jet from the nozzle. Two parallel auxiliary electrodes made of copper foil were placed beside the collector and connected to an alternating current (AC) power supply, which can adjust the driving force acting on the fiber during the dropping process. The nozzle-to-collector distance was adjusted to vary from 0–50 mm, and the moving speed of the substrate was adjusted from 0–400 mm min^{-1}. The microstructure was characterized by an image measurement instrument (Rational VMS-3020H, Dongguan, China).

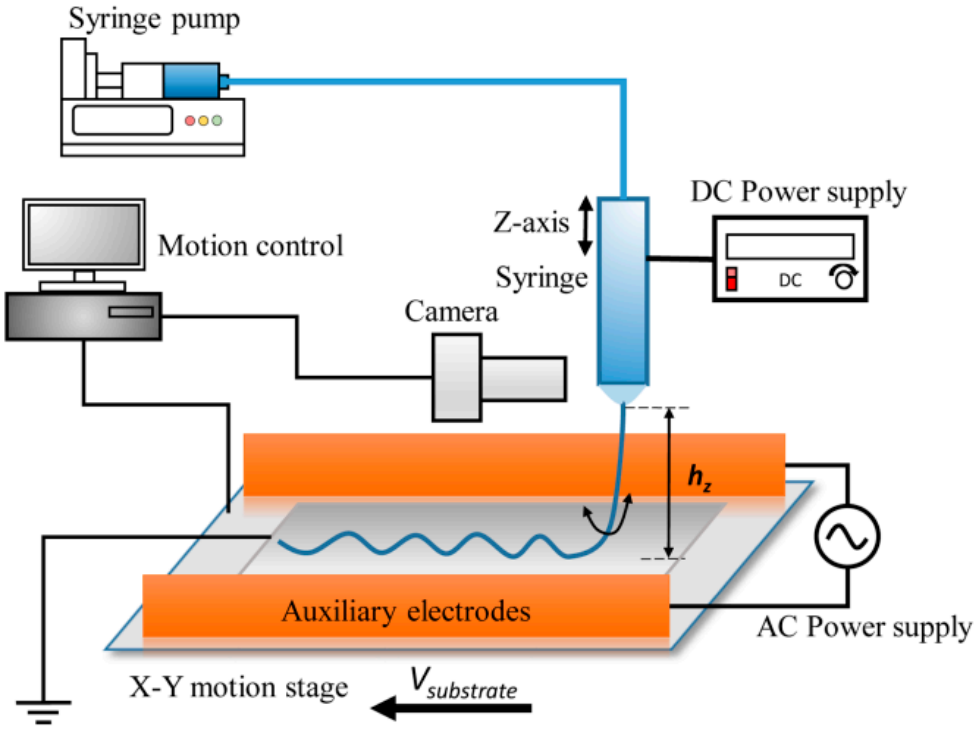

Figure 1. Schematic diagram of wavy-direct-writing.

3. Results and Discussion

Low voltages were applied to the auxiliary electrodes; the AC voltage was set to below 300 V and the DC voltage was lower than 1.5 kV. The low voltage AC–DC coupling electric field constrains the bending of the jet, making it controllable. Therefore, WDW is able to directly write high-resolution serpentine patterns (Figure 2). In the WDW process, the frequency of serpentine patterns is approximately equal to the frequency of AC electric field and the amplitude of the patterns depends linearly on the applied AC voltage value (Figure 3). The pattern wavelength can be controlled precisely by changing the speed of the collector and frequency of the AC voltage, as shown in Figure 2b,d and Table 1.

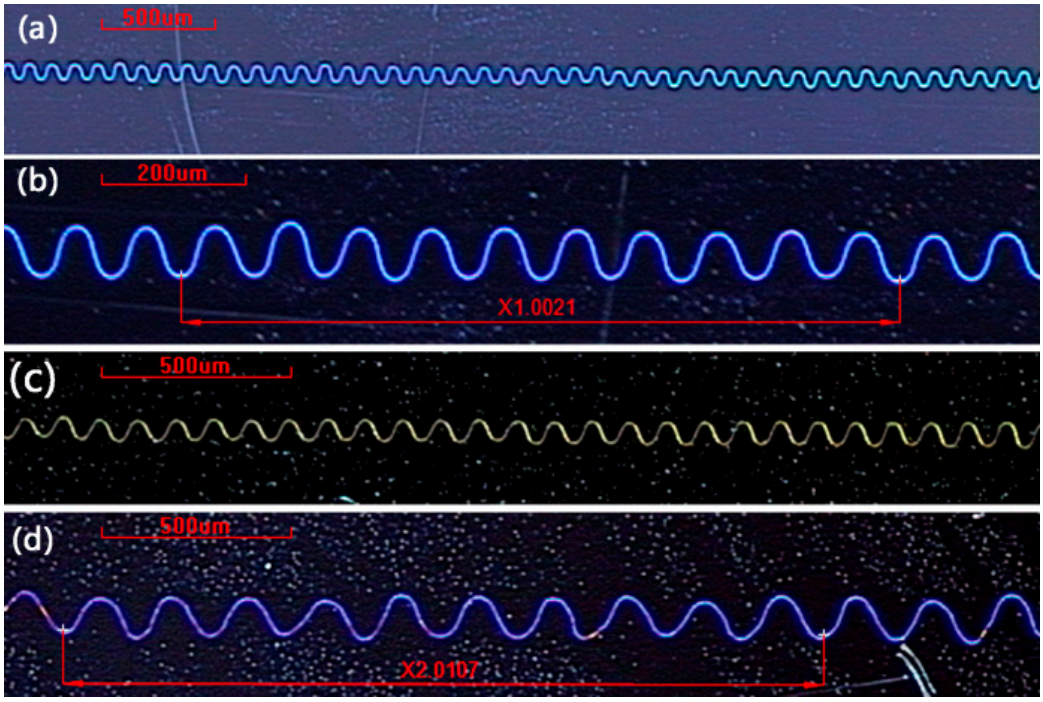

Figure 2. Optical images of the morphology of the serpentine microstructure with different amplitude and frequency of AC voltage applied as well as different substrate velocities: (**a**,**b**) 240 V, 50 Hz, 5 mm/s; (**c**) 180 V, 50 Hz, 5 mm/s; (**d**) 300 V, 60 Hz, 12 mm/s. The solution concentration of (a–c) is 8% and (d) is 6%. All of them were deposited in the following conditions: DC voltage 1.3 kV, auxiliary electrode-to-collector distance 7 mm, nozzle-to-substrate distance 5 mm.

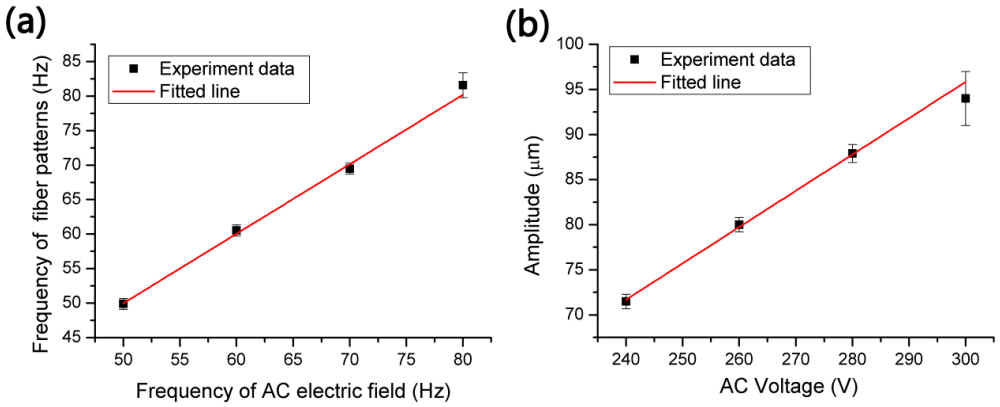

Figure 3. (**a**) Correlation between fiber patterns frequency and AC electric field frequency, and the nanofibers deposited in the following conditions: AC voltage 300 V, DC voltage 1.3 kV, PEO concentration 8%, electrode-to-collector distance 5 mm, collector speed 5 mm/s and the nozzle to auxiliary electrodes distance is 6 mm; (**b**) Correlation between fiber patterns amplitude and AC voltage. The parameters are the same as (a), but the nozzle to auxiliary electrodes distance is 7 mm and the frequency of AC voltage applied is 50 Hz.

Table 1. The wavelength (λ) of serpentine structures deposited with different frequency of the AC voltage and different velocity of substrate. The values correspond to the mean wavelength of each serpentine pattern by measuring every ten waveforms.

Velocity of substrate	λ (μm) at AC 40 Hz	λ (μm) at AC 50 Hz	λ (μm) at AC 60 Hz	λ (μm) at AC 70 Hz
5 mm/s	125.16	100.21	83.53	71.58
8 mm/s	200.39	160.34	133.50	114.55
12 mm/s	301.60	241.28	201.07	171.98

This method differs from traditional ES in that the jetted liquid fiber is pulled by a combination of the DC and AC electrical field forces, and the low voltage AC–DC coupling electric field constrains the bending of the jet to make it controllable. WDW permits direct writing of small size complex serpentine patterns, because the formerly unstable jet can be precisely oriented and positioned. Additionally, unlike conventional drop-on-demand type jet printing technique [10], WDW can print the serpentine patterns in continuous jet mode. Therefore, it is believed that WDW can achieve low cost, high precision fabrication of flexible/stretchable electronics [18,32]. Moreover, we observed that the serpentine structures deposited with different parameters show different structural colors under irradiation of light. The structural colors may be attributed to the effect of scattered light or thin-film interference [33,34].

In order to explain the steady low voltage WDW process, it is necessary to briefly examine the dynamics of WDW. There is no horizontal component of the DC electric field because the space electric field distribution results from the superposition of vertical DC and horizontal AC electric fields. When the nozzle is close to the auxiliary electrodes, the AC electric field force is dominant and the swing of the charged jet can be strongly controlled. Although the change in electric field lags behind the change in applied AC voltage, the frequency and trend are the same. The wavelength of the electromagnetic wave, λ_E, is calculated with:

$$\lambda_E = \frac{C}{f_E} \tag{1}$$

where C is the speed of light and f_E is the frequency of the AC electric field. At very low frequencies AC electric field, λ_E is much smaller than the horizontal distance between nozzle and auxiliary electrodes D_{n-e}. Under these conditions, the electric field can be considered as a quasi-stationary electromagnetic field.

Under low AC voltage and small angle conditions, for any given AC-electric field force and elasticity of the jet, the viscous damping result from the relative motions between the charged jet and substrate are the dominant factors in the horizontal direction. The movement of the charged jet in the horizontal direction is nearly parallel with the AC-electric field, and it can be described using the (sinusoidal) driven damped harmonic oscillator model:

$$m\ddot{x}_{(t)} + c\dot{x}_{(t)} + kx_{(t)} = F_0 \sin(2\pi f_E t) \tag{2}$$

with m being the effective mass of the charged jet, x is the displacement of jet in horizontal direction parallel with the AC-electric field, c is the damping coefficient, k is the spring constant, and F_0 is the driving force resulting from the AC electric field. F_0 is calculated as follows:

$$F_0 = qE_0 \tag{3}$$

where q is the value of the electrostatic charge of the jet and E_0 is the peak value of AC electric field. The steady state solution can be written as:

$$x_{(t)} = Xsin\left(2\pi f_E t + \phi\right) \tag{4}$$

The result states that the charged jet will oscillate at the same frequency, f_{E}, as the applied AC electric field force, but with a phase shift. The phase shift, ϕ, is defined by the following formula:

$$\phi = arctan\left(\frac{-c\omega}{\mathrm{k} - m\omega^2}\right) \tag{5}$$

$$\omega = 2\pi f_E \tag{6}$$

The amplitude of the vibration, X, is defined by the following formula:

$$X = \frac{qE_0}{\sqrt{\left(k - m\omega^2\right)^2 + \left(c\omega^2\right)}} \tag{7}$$

The result shows that X is proportional to the value of E_0. Because E_0 depends linearly on the applied AC voltage value U_{ac}, X is proportional to U_{ac}:

$$X \propto U_{ac} \tag{8}$$

When the collector moves slowly, the mechanical drawing force is so small that it has little impact on the bending of the jet and can be considered to be an equilibrium state of external force in the direction parallel with the speed of the collector. Therefore, under this condition, the "wave velocity" of serpentine patterns is equal to collector's speed and the pattern wavelength, λ, can be calculated as follows:

$$\lambda = \frac{v_{substrate}}{f_E} \tag{9}$$

Using the formulas above, the predicted results are in good agreement with the experimental ones (as shown in Figure 3 and Table 1) and support our model. Therefore, these formulas are effective for describing the stable wavy direct-writing process under low AC voltage and small angle conditions to some extent. Moreover, it means that we can control the frequency, amplitude and wavelength of serpentine patterns accurately by changing the frequency and amplitude of the AC voltage, and the velocity of substrate.

Moreover, in some specific experiments we observed that the serpentine structures turned into a small wavelength "Ω"-like pattern at low collector speeds (Figure 4). The detailed mechanism of this is not clear to us, and only some tentative explanations could be given. The liquid jet carries a positive charge from the spinneret as it is ejected from the apex of the Taylor cone. When charged nanofibers are deposited on the collector, the carried charge would be transferred to the ground. The charge density of the deposited nanofibers would then decrease with deposition time, so the residual charge density distribution of deposited nanofibers was uneven. Under low substrate speed conditions, the fibers are too dense to neglect the effects of the Coulomb forces between them. The repulsive forces from the residual charges cause the jets to deposit as far from each other as possible. Thus, the serpentine pattern assumed a "Ω" pattern.

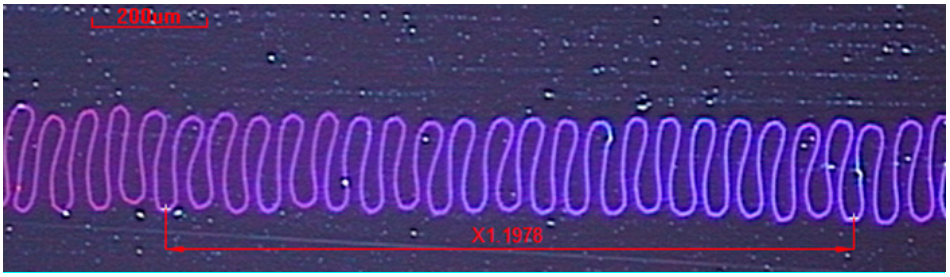

Figure 4. The serpentine structures turned into a small wavelength "Ω"-like pattern at low collector speed.

In the previous section, only an AC electric field perpendicular to the velocity of collector was applied to the charged jet. However when using an AC electric field not perpendicular to the velocity of collector, the serpentine pattern will turn to be lopsided or saw tooth serpentine pattern, as shown in Figure 5.

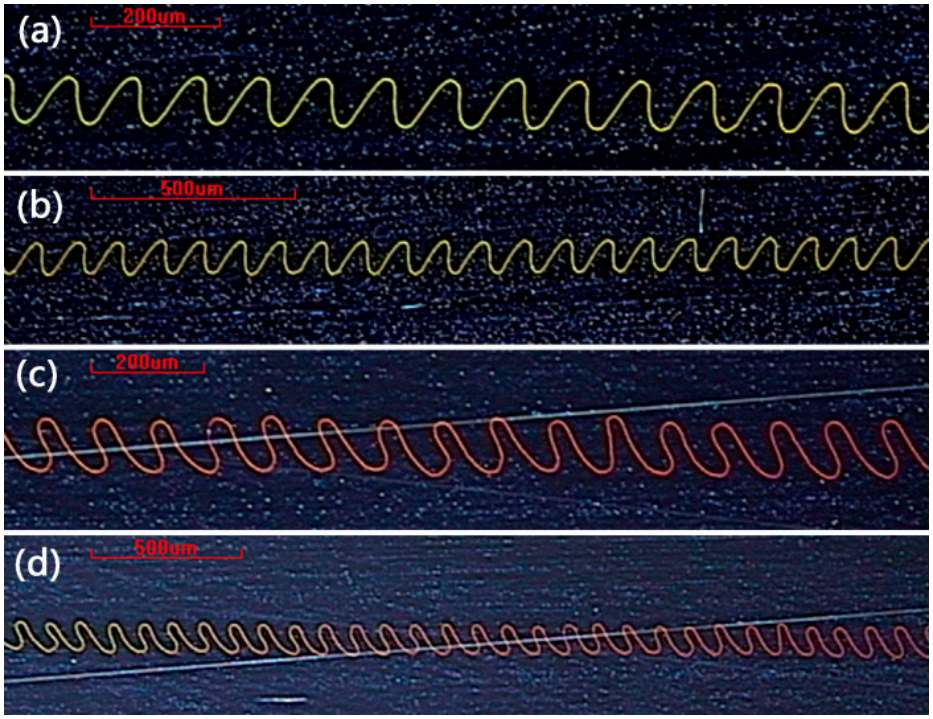

Figure 5. The typical lopsided patterns direct-write with the help of an AC electric field not perpendicular to the velocity of collector. DC voltage 1.3 kV, AC voltage 300 V, 50 Hz, nozzle-to-substrate distance 5 mm, 8% PEO.

4. Conclusions

The low-voltage AC–DC coupling electric field allows for a better control of pattern nanofibers. Small-scale serpentine patterns were made long and uniform. The size and shape can be adjusted by changing the speed of the collector and the frequency and amplitude of the AC voltage applied. Furthermore, because an arbitrary function can be decomposed into a Fourier series, which is a sum of sine and cosine waves, the low voltage WDW has the potential to direct-write any complex wave

pattern. This fabrication ability will permit the use of electrospun-nanofibers-based wiring of structural and functional components in microelectronics, MEMS, sensor, and micro optoelectronics devices.

Acknowledgments

This work was financially supported by National Natural Science Foundation of China (51305084), Project on the Integration of Industry, Education and Research of Dongguan City (No. 2013509109101), Guangdong Innovative Research Team Program (No. 201001G0104781202), Guangdong Provincial Key Laboratory Construction Project of China (Grant No. 2011A060901026), Key Joint Project of National Natural Science Foundation of China (Grant No. U1134004), China Post-Doctoral Science Foundation (125032).

Author Contributions

Feiyu Fang, Ziming Zhu, Peixuan Wu and Han Wang conceptualized the work. Feiyu Fang pursued most of the experimental work. Xin Chen, Zefeng Du, Peixuan Wu and Xindu Chen helped with the materials preparation and measurements. Feiyu Fang and Peixuan Wu completed the manuscript with input from all other authors and critically reviewed the manuscript. All the authors are joined in the extensive discussions and data analysis.

Conflicts of Interest

The authors declare no conflict of interest.

References

1. Kim, D.H.; Lu, N.; Ma, R.; Kim, Y.S.; Kim, R.H.; Wang, S.; Wu, J.; Won, S.M.; Tao, H.; Islam, A.; *et al*. Epidermal electronics. *Science* **2011**, *333*, 838–843. [CrossRef] [PubMed]
2. Song, Y.M.; Xie, Y.; Malyarchuk, V.; Xiao, J.; Jung, I.; Choi, K.J.; Liu, Z.; Park, H.; Lu, C.; Kim, R.H.; *et al*. Digital cameras with designs inspired by the arthropod eye. *Nature* **2013**, *497*, 95–99. [CrossRef] [PubMed]
3. Xu, S.; Zhang, Y.; Cho, J.; Lee, J.; Huang, X.; Jia, L.; Fan, J.A.; Su, Y.; Su, J.; Zhang, H.; *et al*. Stretchable batteries with self similar serpentine interconnects and integrated wireless recharging systems. *Nat. Commun.* **2013**, *4*, 1543. [CrossRef] [PubMed]
4. Yu, D.; Wang, S.; Ye, L.; Li, W.; Zhang, Z.; Chen, Y.; Zhang, J.; Peng, L.M. Electroluminescence from serpentine carbon nanotube based light emitting diodes on quartz. *Small* **2014**, *10*, 1050–1056. [CrossRef] [PubMed]
5. Gutruf, P.; Walia, S.; Nur Ali, M.; Sriram, S.; Bhaskaran, M. Strain response of stretchable micro electrodes: Controlling sensitivity with serpentine designs and encapsulation. *Appl. Phys. Lett.* **2014**, *104*, 021908. [CrossRef]
6. Tseng, A.A.; Chen, K.; Chen, C.D.; Ma, K.J. Electron beam lithography in nanoscale fabrication: recent development. *IEEE Trans. Electron. Pack. Manuf.* **2003**, *26*, 141–149. [CrossRef]
7. Tseng, A.A. Recent developments in nanofabrication using focused ion beams. *Small* **2005**, *1*, 924–939. [CrossRef] [PubMed]

8. Salaita, K.; Wang, Y.; Mirkin, C.A. Applications of dip pen nanolithography. *Nature Nanotech.* **2007**, *2*, 145–155. [CrossRef] [PubMed]
9. Singh, M.; Haverinen, H.M.; Dhagat, P.; Jabbour, G.E. Inkjet printing process and its applications. *Adv. Mater.* **2010**, *22*, 673–685. [CrossRef] [PubMed]
10. Park, J.U.; Hardy, M.; Kang, S.J.; Barton, K.; Adair, K.; Mukhopadhyay, D.K.; Lee, C.Y.; Strano, M.S.; Alleyne, A.G.; Georgiadis, J.G.; *et al.* High resolution electrohydrodynamic jet printing. *Nat. Mater.* **2007**, *6*, 782–789. [CrossRef] [PubMed]
11. Di Benedetto, F.; Camposeo, A.; Pagliara, S.; Mele, E.; Persano, L.; Stabile, R.; Cingolani, R.; Pisignano, D. Patterning of light emitting conjugated polymer nanofibres. *Nature Nanotech.* **2008**, *3*, 614–619. [CrossRef] [PubMed]
12. Camposeo, A.; Persano, L.; Pisignano, D. Light-Emitting electrospun nanofibers for nanophotonics and optoelectronics. *Macromol. Mater. Eng.* **2013**, *298*, 487–503. [CrossRef]
13. Lee, S.W.; Lee, H.J.; Choi, J.H.; Koh, W.G.; Myoung, J.M.; Hur, J.H.; Park, J.J.; Cho, J.H.; Jeong, U. Periodic array of polyelectrolyte gated organic transistors from electrospun poly(3-hexylthiophene) nanofibers. *Nano Lett.* **2010**, *10*, 347–351. [CrossRef] [PubMed]
14. Persano, L.; Dagdeviren, C.; Su, Y.; Zhang, Y.; Girardo, S.; Pisignano, D.; Huang, Y.; Rogers, J.A. High performance piezoelectric devices based on aligned arrays of nanofibers of poly(vinylidenefluoride co trifluoroethylene). *Nat. Commun.* **2013**, *4*, 1633. [CrossRef] [PubMed]
15. Miao, Y.E.; Fan, W.; Chen, D.; Liu, T. High performance supercapacitors based on hollow polyaniline nanofibers by electrospinning. *ACS Appl. Mater. Inter.* **2013**, *5*, 4423–4428. [CrossRef] [PubMed]
16. Dzenis, Y. Spinning continuous fibers for nanotechnology. *Science* **2004**, *304*, 1917–1919. [CrossRef] [PubMed]
17. Bisht, G.S.; Canton, G.; Mirsepassi, A.; Kulinsky, L.; Oh, S.; Dunn Rankin, D.; Madou, M.J. Controlled continuous patterning of polymeric nanofibers on three dimensional substrates using low voltage near field electrospinning. *Nano Lett.* **2011**, *11*, 1831–1837. [CrossRef] [PubMed]
18. Min, S.Y.; Kim, T.S.; Kim, B.J.; Cho, H.; Noh, Y.Y.; Yang, H.; Cho, J.H.; Lee, T.W. Large scale organic nanowire lithography and electronics. *Nat. Commun.* **2013**, *4*, 1773. [CrossRef] [PubMed]
19. Sun, B.; Long, Y.Z.; Chen, Z.J.; Liu, S.L.; Zhang, H.D.; Zhang, J.C.; Han, W.P. Recent advances in flexible and stretchable electronic devices via electrospinning. *J. Mater. Chem. C* **2014**, *2*, 1209. [CrossRef]
20. Sun, D.; Chang, C.; Li, S.; Lin, L. Near field electrospinning. *Nano Lett.* **2006**, *6*, 839–842. [CrossRef] [PubMed]
21. Zheng, G.; Li, W.; Wang, X.; Wu, D.; Sun, D.; Lin, L. Precision deposition of a nanofibre by near–field electrospinning. *J. Phys. D* **2010**, *43*, 415501. [CrossRef]
22. Huang, Y.; Duan, Y.; Ding, Y.; Bu, N.; Pan, Y.; Lu, N.; Yin, Z. Versatile, kinetically controlled, high precision electrohydrodynamic writing of micro/nanofibers. *Sci. Rep.* **2014**, *4*, 5949. [CrossRef] [PubMed]
23. Xin, Y.; Reneker, D.H. Hierarchical polystyrene patterns produced by electrospinning. *Polymer* **2012**, *53*, 4254–4261. [CrossRef]

24. Sun, B.; Long, Y.Z.; Liu, S.L.; Huang, Y.Y.; Ma, J.; Zhang, H.D.; Shen, G.; Xu, S. Fabrication of curled conducting polymer microfibrous arrays via a novel electrospinning method for stretchable strain sensors. *Nanoscale* **2013**, *5*, 7041–7045. [CrossRef] [PubMed]
25. Yu, J.; Qiu, Y.; Zha, X.; Yu, M.; Yu, J.; Rafique, J.; Yin, J. Production of aligned helical polymer nanofibers by electrospinning. *Eur. Polym. J.* **2008**, *44*, 2838–2844. [CrossRef]
26. Han, T.; Reneker, D.H.; Yarin, A.L. Buckling of jets in electrospinning. *Polymer* **2007**, *48*, 6064–6076. [CrossRef]
27. Kessick, R.; Tepper, G. Microscale polymeric helical structures produced by electrospinning. *Appl. Phys. Lett.* **2004**, *84*, 4807. [CrossRef]
28. Ding, Y.; Duan, Y.; Huang, Y.A. Electrohydrodynamically printed, flexible energy harvester using *in situ* poled piezoelectric nanofibers. *Energy Technol.* **2015**, *3*, 351–358. [CrossRef]
29. Duan, Y.Q.; Huang, Y.A.; Yin, Z.P.; Bu, N.B.; Dong, W.T. Non-wrinkled, highly stretchable piezoelectric devices by electrohydrodynamic direct-writing. *Nanoscale* **2014**, *6*, 3289–3295. [CrossRef] [PubMed]
30. Pagliara, S.; Camposeo, A.; Mele, E.; Persano, L.; Cingolani, R.; Pisignano, D. Enhancement of light polarization from electrospun polymer fibers by room temperature nanoimprint lithography. *Nanotechnology* **2010**, *21*, 966–971. [CrossRef] [PubMed]
31. Persano, L.; Camposeo, A.; Pisignano, D. Active polymer nanofibers for photonics, electronics, energy generation and micromechanics. *Prog. Polym. Sci.* **2015**, *43*, 48–95. [CrossRef]
32. Huang, S.; Zhao, C.; Pan, W.; Cui, Y.; Wu, H. Direct writing of half-meter long CNT based fiber for flexible electronics. *Nano Lett.* **2015**, *15*, 1609–1614. [CrossRef] [PubMed]
33. Kuwayama, H.; Matsumoto, H.; Morota, K.; Minagawa, M.; Tanioka, A. Control over color of nanotextured coatings by electrospray deposition. *Sen-Ito Kogyo* **2008**, *64*, 1–4. [CrossRef]
34. Matsapey, N.; Faucheu, J.; Flury, M.; Delafosse, D. Color effects of nanotextured aluminum surfaces: Characterization and modeling of optical behavior. *Adv. Eng. Mater.* **2014**, *17*, 45–51. [CrossRef]